

---

## Supplementary information

---

# Modelling the impact of testing, contact tracing and household quarantine on second waves of COVID-19

---

In the format provided by the  
authors and unedited

# Supplementary Material: Modeling the impact of testing, contact tracing and household quarantine on second waves of COVID-19

Alberto Aleta, David Martín-Corral, Ana Pastore y Piontti, Marco Ajelli, Maria Litvinova, Matteo Chinazzi, Natalie E. Dean, M. Elizabeth Halloran, Ira M. Longini, Jr., Stefano Merler, Alex Pentland, Alessandro Vespignani, Esteban Moro & Yamir Moreno

July 16, 2020

## Contents

<b>1 Mobility data</b>	<b>2</b>
<b>2 Network structure</b>	<b>2</b>
2.1 Agents . . . . .	2
2.2 Contacts . . . . .	3
2.3 Social distancing policies . . . . .	4
2.4 Calibration of intra-layer links . . . . .	4
<b>3 SARS-CoV-2 transmission model</b>	<b>5</b>
3.1 Estimation of the effective reproduction number . . . . .	7
3.2 Strategy implementation . . . . .	8
<b>4 Distribution of infections</b>	<b>9</b>
<b>5 Household attack rate</b>	<b>10</b>
<b>6 Sensitivity analysis</b>	<b>10</b>
6.1 Model parameters . . . . .	10
6.2 Symptomatic detection rate . . . . .	10
6.3 Contact tracing delay . . . . .	11
6.4 Effect of different attack rates . . . . .	11
<b>7 School reopening</b>	<b>11</b>
<b>8 Soft distancing measures and transmissibility reduction</b>	<b>11</b>

# 1 Mobility data

The mobility data was obtained from Cuebiq, a location intelligence and measurement company. The dataset consists of anonymized records of GPS locations from users that opted-in to share the data anonymously in the Boston metropolitan area over a period of 6 months, from October 2016 to March 2017. Data was shared in 2017 under a strict contract with Cuebiq through their Data for Good program where they provide access to de-identified and privacy-enhanced mobility data for academic research and humanitarian initiatives only. All researchers were contractually obligated to not share data further or to attempt to de-identify data. Mobility data is derived from users who opted in to share their data anonymously through a General Data Protection Regulation (GDPR) and California Consumer Privacy Act (CCPA) compliant framework.

From the data we extracted the “stays”, as the places where anonymous users stayed (stopped) for at least 5 minutes. Some of the stays happen within places (Points of Interest). We use a dataset of 86k Points of Interest in the Boston metropolitan area collected using the Foursquare API. Stays are then aggregated at place level. Finally we estimate the home Census Block Group of the anonymous users as that in which they are more likely located during nighttime. This results in a dataset of the places people stayed including the points of interest that anonymous users visited and the most likely census block group of where the device owner lives.

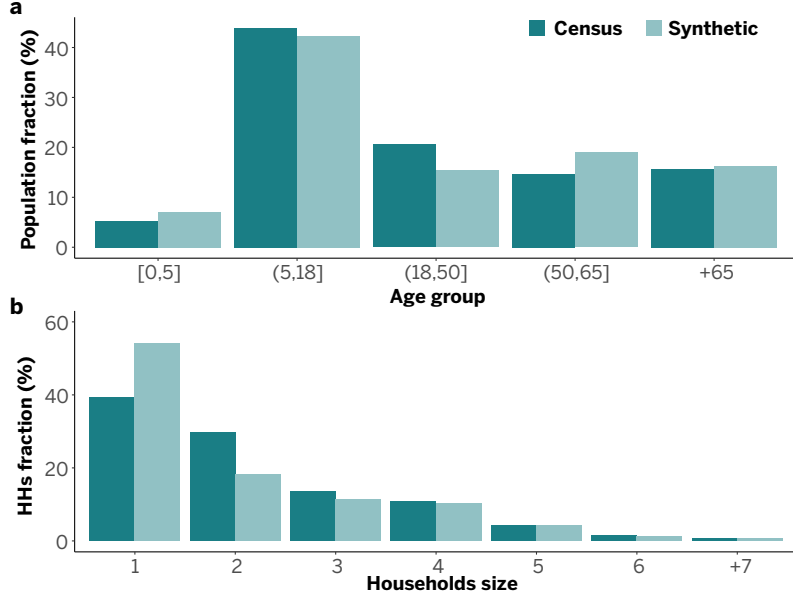
# 2 Network structure

## 2.1 Agents

Our population consists of two different sub-populations, adults and children. Adults are sampled from anonymous individuals in the mobility data collected by Cuebiq, each adult is associated with a home location assigned to a US Census block group which is provided by our location data provider. With this data we designed a population building pipeline that consists of three steps.

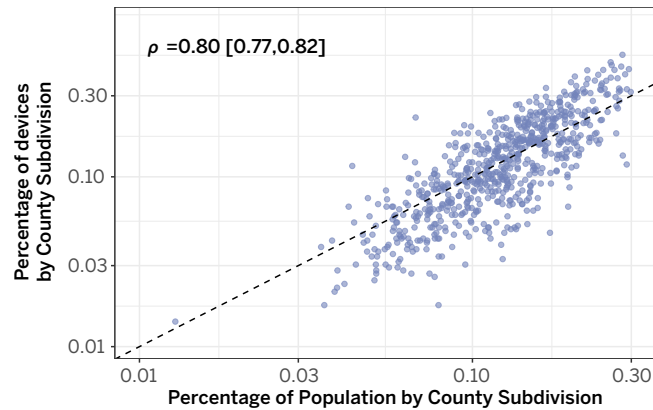
- First step, we build synthetically the number of households, their size and the presence of children based on our adult population and the US Census [1] tables B11016 (Household Type by Household Size) and B11003 (Family Type by Presence and Age of Own Children)
- Second step, we assign adults to households and in case of presence of children we generate them up to reach the size of the household assigned in the first step.
- And final step, we assign ages to nodes using table B01001 (Ages by Sex) of age distribution within the Census Block Group.

This process generates our synthetic population consisting of 85k agents (2% of the population in the Boston Metropolitan Area), 64k (75%) of them are adults and 21k (25%) are children. Age groups are distributed as follows: 6,027 (7%) agents for the age group between zero and five years old, 16,250 (18.9%) agents for the age group between six and eighteen years old, 36,207 (42.2%) agents for the age group between nineteen and fifty years old, 13,176 (15.4%) agents for the age group between fifty one and sixty five years old, and final group, 13,945 (16.2%) agents for the age group between sixty six and older. All of agents together form 43,167 households distributed as follows: 23,293 (53.9%) households with only one agent, 7,886 (18.2%) with two agents, 4,959 (11.4%) with three agents, 4,486 (10.4%) with four agents, 1,784 (4.1%) with five agents, 514 (1.2%) with six agents, and finally, 245 (0.5%) with seven agents. In Figure 1 we can see the comparison of our synthetic population against census data.



Supplementary Figure 1: Age groups and households demographics compared against US Census data. (a) Age groups distribution. (b) Households size distribution.

Our sample from devices is very representative of the population in the Boston area. As we can see in Figure 2, population and number of anonymous devices detected in the real data by census area are highly correlated:  $\rho = 0.8$  (Pearson correlation) with a CI between 0.77 and 0.82 for county subdivisions.



Supplementary Figure 2: The correlation between the population for each county subdivision and the number of devices in our dataset.

## 2.2 Contacts

In the unmitigated scenario, our network has a total number of 5,029,888 unique daily contacts, 3,924,694 (78%) of them in the community layer obtained using the mobility data, 160,748 (3%) and 944,446 (19%) are synthetically built for the household and school layers, respectively. The community layer is based on estimation of co-presence of two devices in Points of Interest visited by the anonymous users (see Methods in the main paper). Points of interest (POIs) are categorized using the Foursquare taxonomy of places which has ten main categories: Art & Entertainment (4.4%), Colleges & Universities (4.8%), Food (16.7%), Nightlife Spots (3.9%), Outdoors & Recreation (10.6%), Professional & Other Places (23.7%), Shops & Services (29.1%) and Travel & Transport (6.4%), and 638 subcategories. See [2] for a complete list of them.

## 2.3 Social distancing policies

We simulated two different scenarios for social distancing policies. This produces three contact networks: i) *baseline*, ii) *medium closure*, and iii) *non-essential closure*, as we see it in more detail in Table 1. Schools are closed in the medium and non-essential closure, but both policies differ in the number of places kept open in the community layer. In Table 2 we can see the distribution of POIs, by main Foursquare category, that remain open during each social distancing policy. In the baseline scenario, we keep all the categories and thus the average number of contacts in the community layer is 63 (median 47, [15-150] 90% confidence interval), with few anonymous individuals having a large number of contacts (that could eventually lead to super-spreading events). In the medium closure scenario, POIs in the Art & Entertainment, Restaurants and Nightlife categories are closed; this drastically reduces the average number of contacts to 27 (median 15, [0-92] 90%CI). Lastly, when all non-essential places are closed, we only keep open the following subcategories: Hospital, Salon / Barbershop, Grocery Store, Dispensary, Supermarket, Pet Store, Pharmacy, Urgent Care Center, Dry Cleaner, Drugstore, Maternity Clinic, Medical Supply, and Gas Station. In this situation, the average number of contacts is reduced to 6 (median 0, [0-29] 90%CI). The distribution for the number of contacts in the community layer in these three scenarios is shown in Figure 3.

Layers	Baseline			Medium closure			Non-essential closure		
	Contacts	%.		Contacts	%	% Diff.	Contacts	%	% Diff.
Community	3,924,694	78		1,378,054	27.4	-72.6	357,144	7.1	-92.9
Households	160,748	3.2		160,748	3.2	0	160,748	3.2	0
Schools	944,446	18.8		0	0	-100	0	0	-100
Total	5,029,888	100		1,538,802	30.6	-69.4	517,892	10.3	-89.7

Supplementary Table 1: Number of daily contacts by layer and social distancing policy.

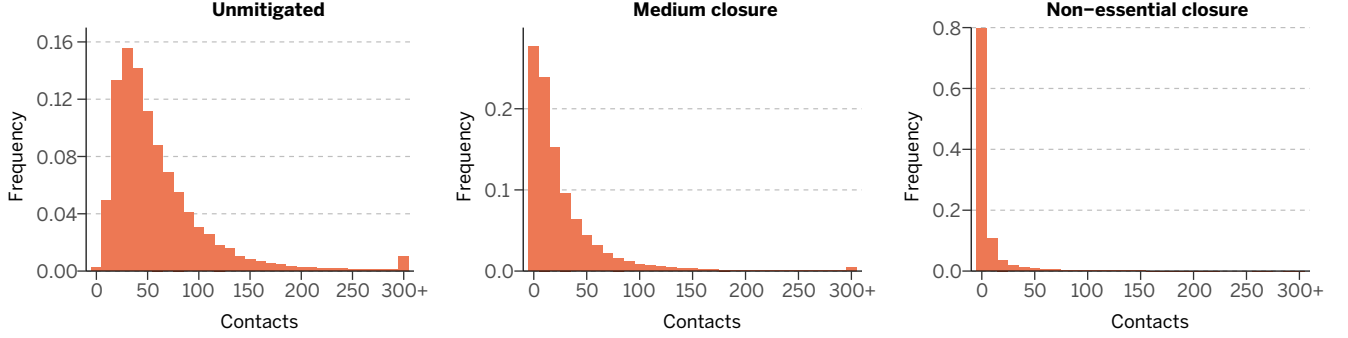
POIs categories	Baseline			Medium closure.			Non-essential closure.		
	Open	%.		Open	%	% Diff.	Open	%	% Diff.
Arts and Entertainment	3,692	4.44		0	0	-100	0	0	-100
Colleges and Universities	4,016	4.83		4,016	4.83	0	0	0	-100
Restaurants	13,860	16.7		0	0	-100	0	0	-100
Nightlife Spots	3,288	3.95		0	0	-100	0	0	-100
Outdoors and Recreation	8,840	10.64		8,840	10.64	0	229	0.27	-97.4
Professional and Other Places	19,692	23.71		19,692	23.71	0	415	0.5	-97.8
Shops and Services	24,310	29.27		24,310	29.27	0	5,139	6.19	-78.8
Travel and Transport	5,370	6.46		5,370	6.46	0	0	0	-100
Total	83,608	100		62,228	74.91	-25.6	5,783	6.96	-93.1

Supplementary Table 2: Number of POIs open in the Community layer by the different social distancing measures and full non-essential closure. Percentages are calculated with respect to the total number of POIs in the baseline.

## 2.4 Calibration of intra-layer links

As described in the main text, we define  $\omega_{ij}$  as the weight associated to the link between node  $i$  and  $j$ .

In the community+workplace layer, we estimate the mean number of daily effective contacts ( $\eta_C$ ) by



Supplementary Figure 3: Degree distribution in the community layer under normal conditions, soft social distancing measures and full non-essential closure.

using  $\omega_{C_{ij}}$ , which is based on the co-presence probability estimation.  $\eta_C$  can thus be calculated as

$$\begin{aligned}\eta_C &= 1/n \sum_{i \in \{1, \dots, n\}} \sum_{j | j \neq i \wedge j \in \{1, \dots, n\}} \omega_{C_{ij}} \\ &= 2.5\end{aligned}$$

By construction, the weights for the household layer were assigned as  $\omega_{H_{ij}} = 1/(h - 1)$ , where  $h$  is the number of household members, so that  $\eta_H = 1$ . Analogously, by construction, for schools we have  $\eta_S = 1$ .

It is important to note that  $\eta_{C,H,S}$  refer to the mean number of daily effective contacts in the synthetic (non-calibrated) network. Based on the analysis of contact survey data from 9 countries [3, 4, 5, 6, 7], the estimated number of daily effective contacts by social setting is 10.86 in community+workplace, 4.11 in household, and 11.41 in school.

To calibrate the weights of intra-layer links ( $\hat{\omega}_l$ ), we associate to each layer a single rescaling factor  $w_l$  such that the mean number of daily effective contacts in that layer matches mean number of daily effective contacts in the corresponding social setting. Therefore, the calibrated mean number of daily effective contacts in the community+workplace layer  $\hat{\eta}_C$  is

$$\begin{aligned}\hat{\eta}_C &= 1/n \sum_{i \in \{1, \dots, n\}} \sum_{j | j \neq i \wedge j \in \{1, \dots, n\}} \omega_{C_{ij}} w_{C+W} \\ &= 1/n \sum_{i \in \{1, \dots, n\}} \sum_{j | j \neq i \wedge j \in \{1, \dots, n\}} \hat{\omega}_{C_{ij}} \\ &= 2.50 \times 10.86 / 2.50 \\ &= 10.86\end{aligned}$$

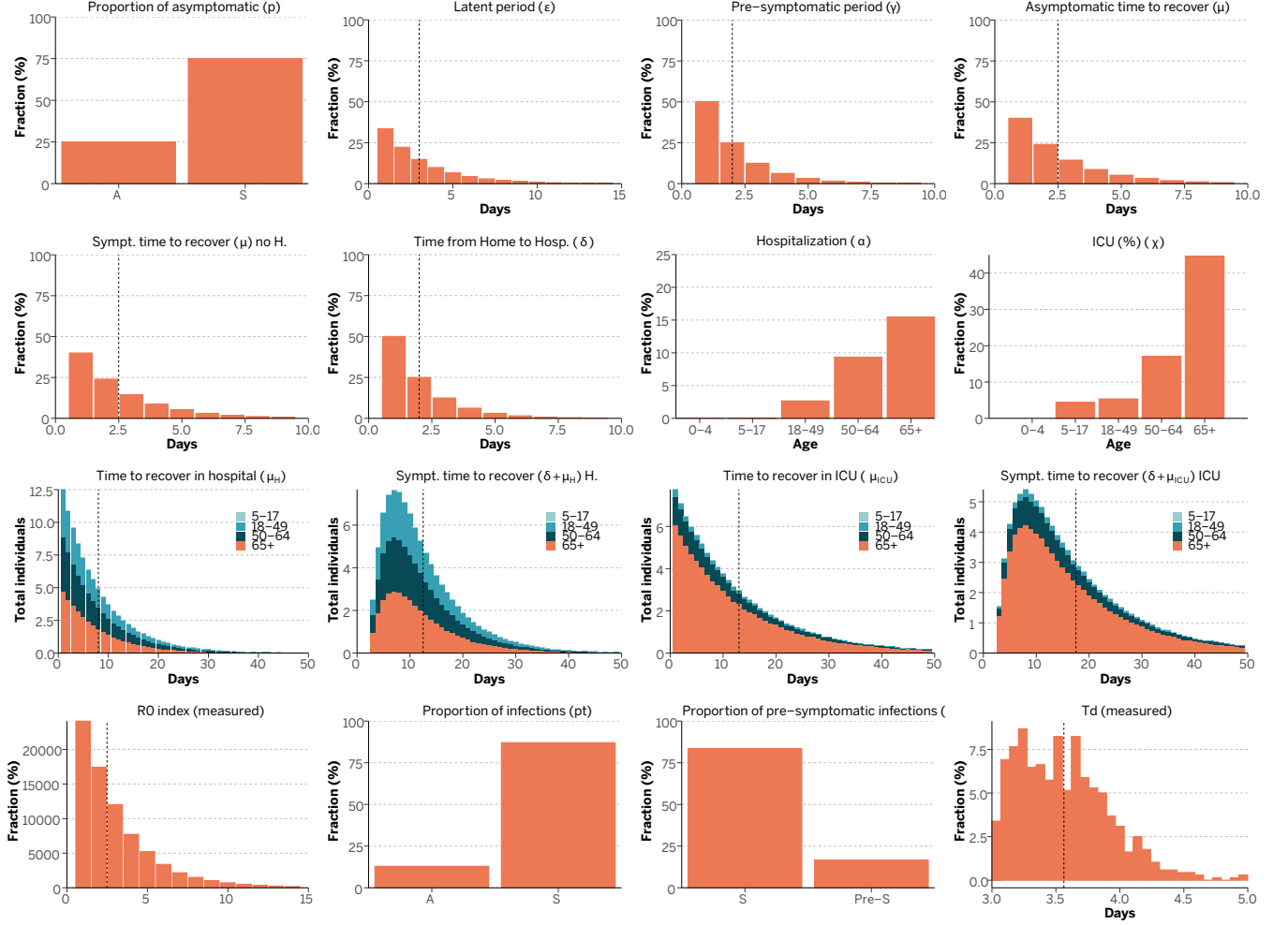
where  $w_{C+W} = 10.86/2.5$ . Analogously for household and school layers we obtain  $w_H = 4.11$  and  $w_S = 11.41$ .

### 3 SARS-CoV-2 transmission model

The values of all the disease parameters used for simulating the transmission dynamics are given in table 3. Figure 4 shows the numerical distributions of these parameters as resulting from simulations of the model.

Parameters	Description	Age group	Value	Ref.
$r$	relative infectiousness of asymptomatic individuals	-	50%	†
$\epsilon^{-1}$	latent period	-	3 days	[8]
$\epsilon'^{-1}$	latent period	-	5 days	[8]
$p$	proportion of asymptomatic	-	25%	[9]
$\gamma^{-1}$	pre-symptomatic period	-	2 days	[8]
$\mu^{-1}$	time to removed/home stay	-	2.5 days	*
$\alpha$	symptomatic case hospitalization ratio (%)	0-4 5-17 18-49 50-64 65+	0.0 0.025 2.672 9.334 15.465	[10]
$\chi$	ICU % among hospitalized	0-4 5-17 18-49 50-64 65+	5.0 5.0 5.38 17.10 44.71	[11]
$\delta^{-1}$	days from home stay to hospital admission	-	2	[12]
$\mu_H^{-1}$	days in hospital	-	8	[10]
$\mu_{ICU}^{-1}$	days in ICU	-	13	[10]
$k$	proportion of presymptomatic transmission	-	15%	[13]
$R_0$	basic reproduction number	-	2.5	†
$\beta$	transmission for symptomatic and asymptomatic individuals	-	$\frac{R_0\mu}{pr+(1-p)/(1-k)}$	
$\beta_S$	transmission for pre-symptomatic individuals	-	$\frac{\beta\gamma k}{\mu(1-k)}$	

Supplementary Table 3: Baseline set of parameters. †: assumed (see Section 6 for sensitivity analysis);\*: calibrated to the generation time  $T_g$ .



Supplementary Figure 4: Model's parameters and distributions summary.

### 3.1 Estimation of the effective reproduction number

We assume that the daily number of new infectious individuals  $C(t)$  at time  $t$  can be approximated as

$$C(t) \approx Pois \left( R(t) \sum_{s=1}^t \phi(s) C(t-s) \right), \quad (1)$$

where  $\phi$  is the generation time distribution and  $R(t)$  is the effective reproduction number at time  $t$ . The generation time is directly measured in the simulations and fitted to a log-normal distribution with mean 6.6 days.

In each single run, the likelihood  $L$  of the observed time series of cases from day 1 to  $T$  is given by

$$L = \prod_{t=1}^T P \left( C(t), R(t) \sum_{s=1}^t \phi(s) C(t-s) \right), \quad (2)$$

where  $P(k, \lambda)$  is the probability mass function of a Poisson distribution. The posterior distribution of  $R(t)$  is then explored using MCMC sampling [14, 15].

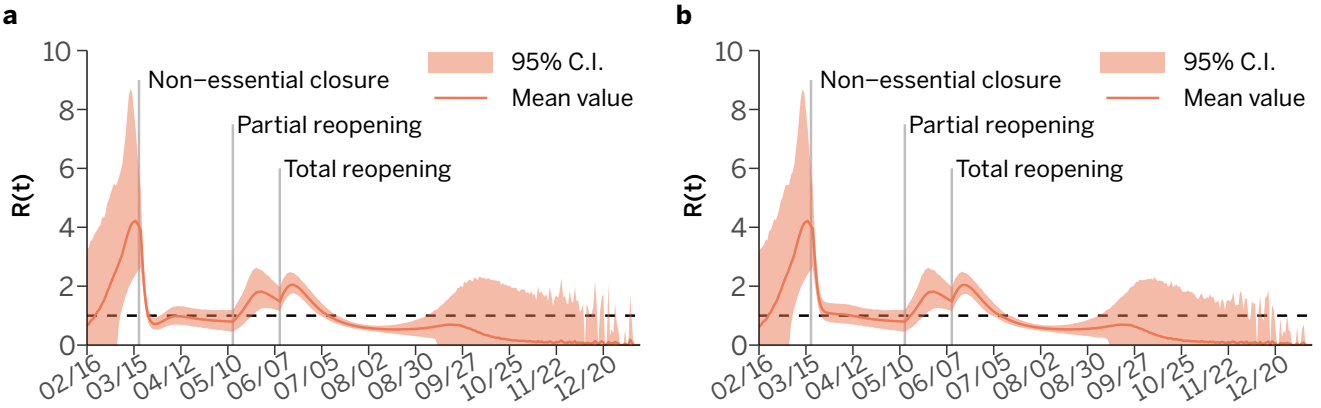
After the implementation of social distancing policies, a certain amount of nodes will be completely disconnected from the system (individuals living alone who lose all their links in the community layer).

Denoting this quantity as  $Z(t)$ , the actual number of infectious individuals that can produce new cases is  $C(t) - Z(t)$ . We modify expression (2) accordingly so that

$$L = \prod_{t=1}^T P \left( C(t), R(t) \sum_{s=1}^t \phi(s) [C(t-s) - Z(t-s)] \right). \quad (3)$$

Note that  $Z(t-s)$  will always be 0 in the unmitigated scenario and larger than zero only in a few steps after the total closure.

In Figure 5 we compare the effective reproduction number estimated using equations (2) and (3). Right after the closure the estimation obtained using (2) shows a small valley followed by an increment of  $R(t)$ . This is produced by nodes that lose all their connections and thus cannot spread the disease at all. Once they recover, since the disease will be still spreading through a small fraction of the system,  $R(t)$  seems to increase. Using equation (3) corrects this problem and  $R(t)$  shows a continuously decreasing trend until the partial reopening.



Supplementary Figure 5: Estimation of the effective reproduction number using equation (2) (panel a) or (3) (panel b). Solid lines represent the mean and the shaded region the 95% C.I.

### 3.2 Strategy implementation

On March 17th all links in the school layer are removed, as well as all links in the community+workplace layer associated to non-essential places. After 8 weeks, all these links in the community+workplace layer are restored, except the ones belonging to restaurants, nightlife, museums, etc (see Section 2.3 above). Lastly, after 4 weeks the rest of the links of the community+workplace layer are added to the system (while schools remain closed). We align the computational step with the real dates so that on March 17th the attack rate in the population is 1.5% in the Figures shown in the main text. In section 6.4 we explore the effect of choosing different attack rates for initializing our simulations.

Then, in the LET scenario, quarantines are applied starting on the same day of the partial reopening (i.e., 8 weeks after the initial closure). We have explored 3 types of quarantines:

- i) A fraction  $qH$  of all the symptomatic individuals is identified after, on average,  $qI$  days of the onset of symptoms. After identification, they are completely isolated in special locations (i.e., outside of their households). A fraction  $qT$  of their contacts are traced and quarantined without testing in special locations where they are also completely isolated.
- ii) A fraction  $qH$  of all the symptomatic individuals is identified after, on average,  $qI$  days of the onset of symptoms. After identification, they are isolated at their homes. A fraction  $qT$  of their contacts are traced and quarantined without testing at their homes.

- iii) A fraction  $qH$  of all the symptomatic individuals is identified after, on average,  $qI$  days of the onset of symptoms. After identification, they are isolated in their households and the rest of the household is set in quarantine (i.e., they cannot contact anyone outside their household). A fraction  $qT$  of their contacts are traced and their households are quarantined without testing.

After 14 days, all individuals isolated or under quarantine are allowed to interact again, regardless of their health status.

In Figure 6, we explore the ICU usage at the peak as a function of the amount of detection ( $qH$ ) and the amount of tracing ( $qT$ ) when symptomatic individuals are identified, on average, in 1, 2 or 3 days ( $qI$ ). The dashed line represents the boundary of ICU saturation. For any pair of  $qT, qH$  values on the left of the dashed line, the burden of ICU usage will surpass the current capacity. Note that the maximum capacity is the same in all cases, but different values of detection and tracing produce a different maximum usage. These results indicate that investing in contact tracing and symptomatic detection is a better strategy than simply multiplying the number of available ICU beds. Indeed, doubling the ICU capacity would only reduce the amount of symptomatic detection necessary by 10%.

We further explore the value of this threshold in Figure 7. We observe that increasing the time of symptomatic detection and isolation increases both the number of symptomatic individuals that have to be detected and the amount of tracing performed. We also note that even though the quarantine of whole households seems to be the best option, isolating and quarantining individuals outside of their households is also a viable strategy. However, as we show next, even though this measure has a lower burden on the families and their individuals economy, it will increase the costs for the overall society.

In Figure 8, we show the maximum number of individuals whose contacts are traced in a single day. Furthermore, note that identifying those individuals as symptomatic also requires testing. Hence, this measure will be proportional to the amount of tests that have to be performed daily (the total number will depend on the positive test rate). Note that even though isolating and quarantining individuals in special locations has a similar effect as doing so in their households from the ICU usage point of view, the number of tracers needed in the former strategy is larger than in the latter. This implies that the amount of testing will also be higher. Added to the cost of creating and managing such special facilities, these results indicate that quarantining whole households is the best strategy overall. However, whenever possible, the possibility of isolating and quarantining single individuals in special locations should be offered to the families who would suffer the most due to the complete quarantining of their household members.

## 4 Distribution of infections

In Figure 9 we show how the infections that are produced for each strategy are distributed across layers. In the unmitigated scenario the disease spreads initially through the community+workplace layer. By the time the incidence peaks (around 04/12) infections are transmitted roughly equally through each layer.

In the LIFT scenario the fraction of infections that take place in households is larger than in the unmitigated one during the first closure. Once places in the community+workplace layer are reopened, the disease starts to spread through that layer again.

Lastly, in the LET strategy, in comparison to the LIFT scenario, we observe a larger fraction of infections within households in the period between partial and total reopening, which is to be expected since symptomatic individuals are forced to stay at home. This suggests that providing special facilities to isolate those individuals will be beneficial for their families.

## 5 Household attack rate

In Figure 10, we explore the secondary attack rate in households. The attack rate in a household, with at least one infected individual, is defined as the fraction of household members (excluding the first infected member) that have suffered the disease. While in the unmitigated scenario this attack rate quickly rises to 80%, in the two other scenarios the situation is slightly different. The initial confinement of individuals at their household initially increases the attack rate, but since the overall burden of the disease is lower by the end of the epidemic, the final attack rate is also lower than in the unmitigated scenario. This also explains why the household attack rate in the LET scenario is small (compared to the other two situations) even though people are forced to stay at home.

## 6 Sensitivity analysis

### 6.1 Model parameters

We conducted a sensitive analysis to study the effects of different percentages of asymptomatic cases, higher transmissibility and higher pre-symptomatic transmission. We consider a scenario where all parameters are kept the same as the unmitigated scenario discussed in the main manuscript with the exception that we consider 50% of cases are asymptomatic (henceforth, set A). We also considered the effect of increasing the pre-symptomatic transmission of the virus, setting  $k = 0.50$  (henceforth, set B) in line with recent observations [16]. Lastly, we test a scenario of higher transmission, where  $R_0 = 3.0$  and the time to hospitalization is increased  $\delta^{-1}$  to 4 days (henceforth, set C).

Figure 11 shows the results for the sensitivity analysis when we consider the unmitigated scenario (a-c) and the LIFT scenario (d-e) for the first two sets of parameters. As we can see, changing these distributions does not affect the total number of infections. Instead, the main change is related to the velocity of propagation. Increasing the pre-symptomatic transmission slightly accelerates the disease, even though the final outcome is fairly similar.

Figure 12 shows the results for the LET scenario where we consider 50% detection of symptomatic cases and different levels of contact tracing: no tracing, 20%, and 40%. The increase of asymptomatic individuals (set A) reduces the effect of contact tracing. Increasing the amount of pre-symptomatic transmission also increases the incidence, something that is expected since individuals will be able to spread more the disease before showing symptoms and being isolated. In any case, in figure 13, we can see that the LET strategy is still feasible with these parameters, signaling that it is quite robust.

We report a similar analysis in figures 14, 15 and 16 for the set of parameters with larger  $R_0$  (set C). As expected, this change yields a higher number of infections. Nonetheless, the overall behavior holds and, even though tracing might need to be slightly increased, the LET strategy is still feasible.

Summarizing, the sensitivity analysis shows that the modeling results presented in the main text are robust to plausible ranges of parameter values for the key time-to-event intervals of COVID-19.

### 6.2 Symptomatic detection rate

In the main text we mainly explored the situation in which 50% of all symptomatic individuals can be detected and their contacts traced, on average, in two days. In Figures 17 and 18 we show the evolution of the system with a detection rate of 30% and 70%, respectively. Once again, our results and conclusions hold.

### 6.3 Contact tracing delay

In the main text we considered that symptomatic individuals could be identified, on average, on two days after the onset of symptoms. However, it was assumed that the contacts of the symptomatic individual could be traced and isolated within that same period of time. In this subsection we explore the effect of needing 1 or 2 days to perform the tracing and isolation of the contacts (figures 19 and 20 respectively). The effect on this delay is fairly small, which is to be expected due to the long incubation period of this disease.

### 6.4 Effect of different attack rates

In Figure 21 we explore the effect of choosing a different initial attack rate for the implementation of the social distancing policies. We observe that the sooner these policies are implemented (i.e., the disease has not spread through the population and thus the attack rate is low) the smaller the first peak of the disease will be. However, once the restrictions are removed, if there is a second wave the peak will be larger. Conversely, if the policies are implemented once a large fraction of the population has already suffered the disease, the second wave of the epidemic will be much milder.

## 7 School reopening

In the main scenarios studied in the paper, once schools are closed they remain so indefinitely. In this section, we explore the consequences of reopening schools on the 15th of September. In figure 22 we show the evolution of the epidemic for the LIFT and LET scenarios under such condition. As we can see, since in the LIFT scenario the peak of the epidemic occurs in July, the effect of reopening schools is negligible. A similar observation can be made in the LET scenario without tracing. However, for the LET scenarios with tracing, since the peak of the epidemic has not faded out by that date, reopening schools produces a small increment on the incidence. Nonetheless, in figure 23 we observe that such increment does not saturate the health care system. This signals that the increase in the number of infections is due to children getting infected, since this group is less likely to require hospitalization.

In figure 24 we explore the affordability of the LET scenario when schools are reopened. In the cases of no tracing and 20% tracing, since the peak of quarantined households is set before September, the reopening does not produce a large increase on the households that have to be set under quarantine. However, in the 40% tracing scenario since the peak is close to the date when schools would reopen, the population under quarantine could pass the 10%. It is important to stress that the role of children in the transmission of SARS-CoV-2 is not yet clear. Several papers indicates a differential susceptibility to the infection as well as a smaller probability of developing symptoms. In principle this might lead smaller role of school reopenings that should be assessed in the presence of firm data on differential forward transmission across different age brackets.

Lastly, in figure 25 we show the household attack rate and the fraction of infections that would take place in each layer. We observe that the household attack rate would remain stable and that the number of infections that would take place in schools will increase above 0.

## 8 Soft distancing measures and transmissibility reduction

In this section we explore the effect that soft social distancing measures, such as wearing masks, increasing the space between individuals in closed places, cleaning more often public spaces, etc. To do so, we reduce

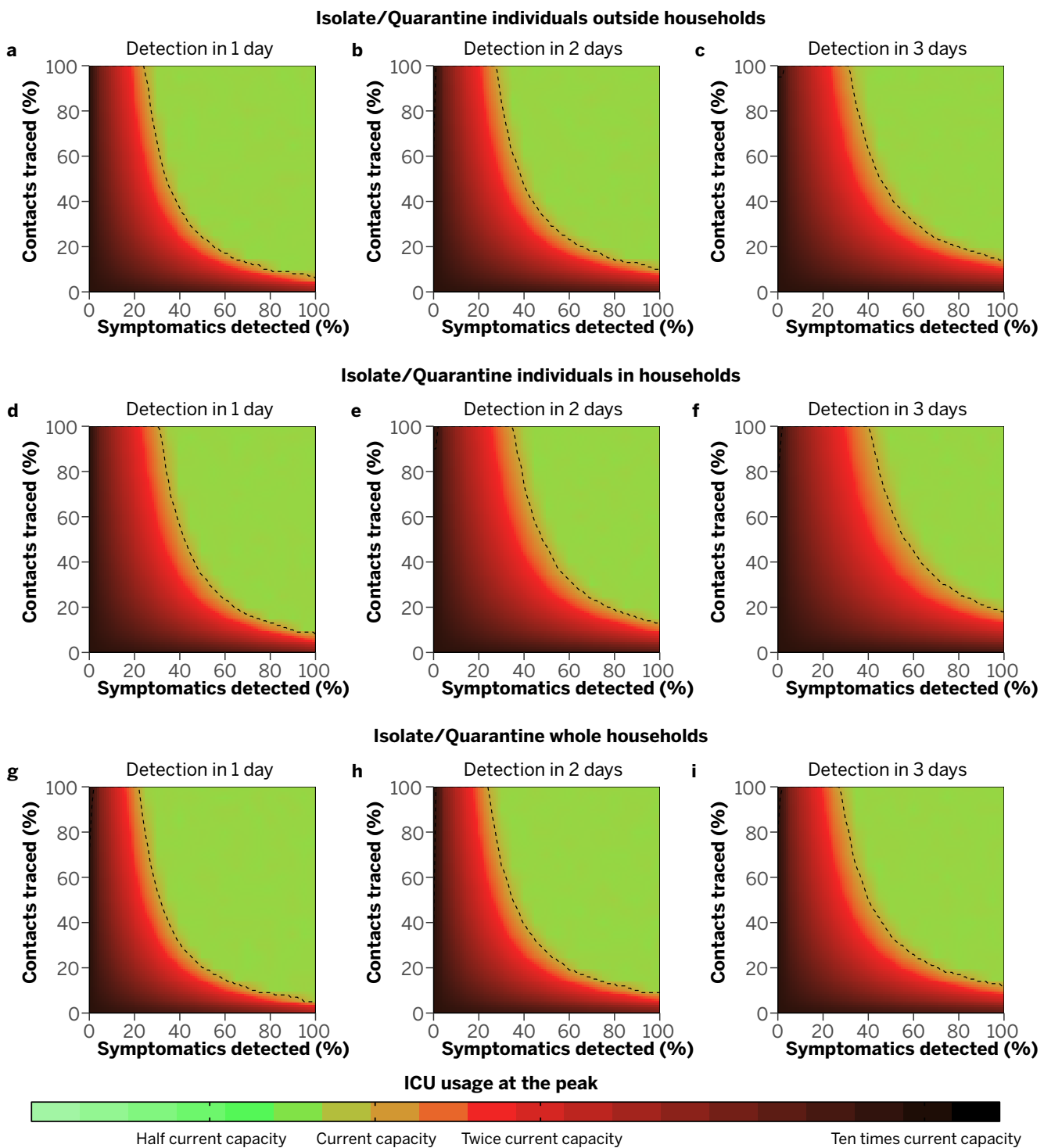
the overall transmissibility of the disease by a certain coefficient since these measures are usually applied to all individuals and not only to the ones affected by the disease.

In figure 26, we show the effect that population-wide measures would have in the LIFT scenario if they are applied on the same date as the total reopening. We observe that even with a 60% reduction the ICU capacity will be surpassed. As such, these measures, on their own, will not be enough to contain the epidemic.

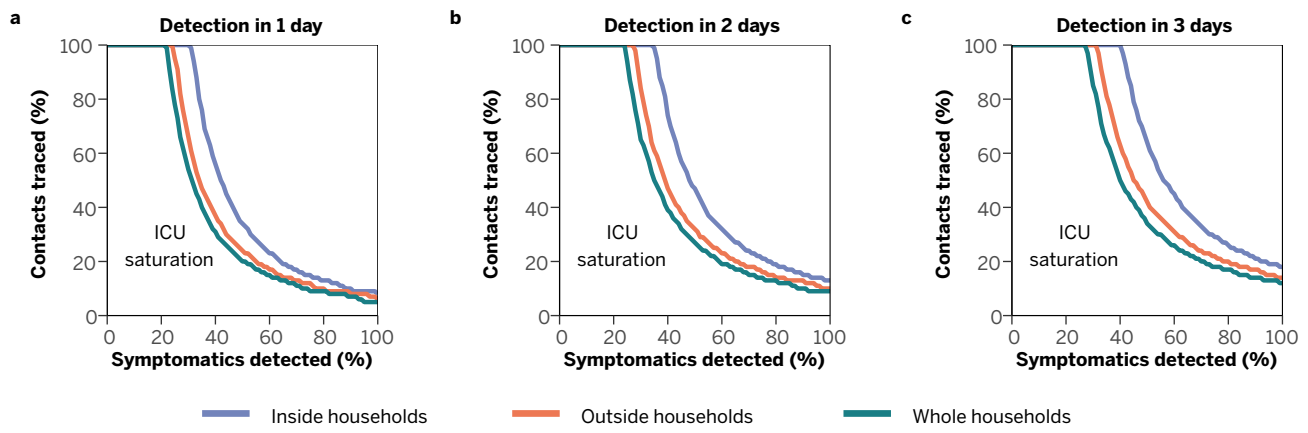
In figure 27, we apply this reduction to the LET scenario with 50% symptomatic detection but without any tracing. We can see that to keep the ICU usage below the threshold a large reduction of at least 60% is needed. Thus, even though these measures can help, they are not enough if only symptomatic individuals are isolated. On the other hand, in figure 28, we analyze the situation in which 20% of the contacts are traced and isolated (note that in the main text the main success scenario requires 40% of contact tracing). In this case the reduction of transmissibility has a dramatic effect, even with just a 20% reduction. Indeed, not only in all the cases analyzed the ICU needs are within the availability limit, but also the fraction of individuals and households that have to be quarantined is much smaller than in the no reduction case. As such, complementing the test and tracing strategy with soft social distancing measures can clearly benefit the containment of the epidemic, specially because less test and tracers will be necessary.

## References

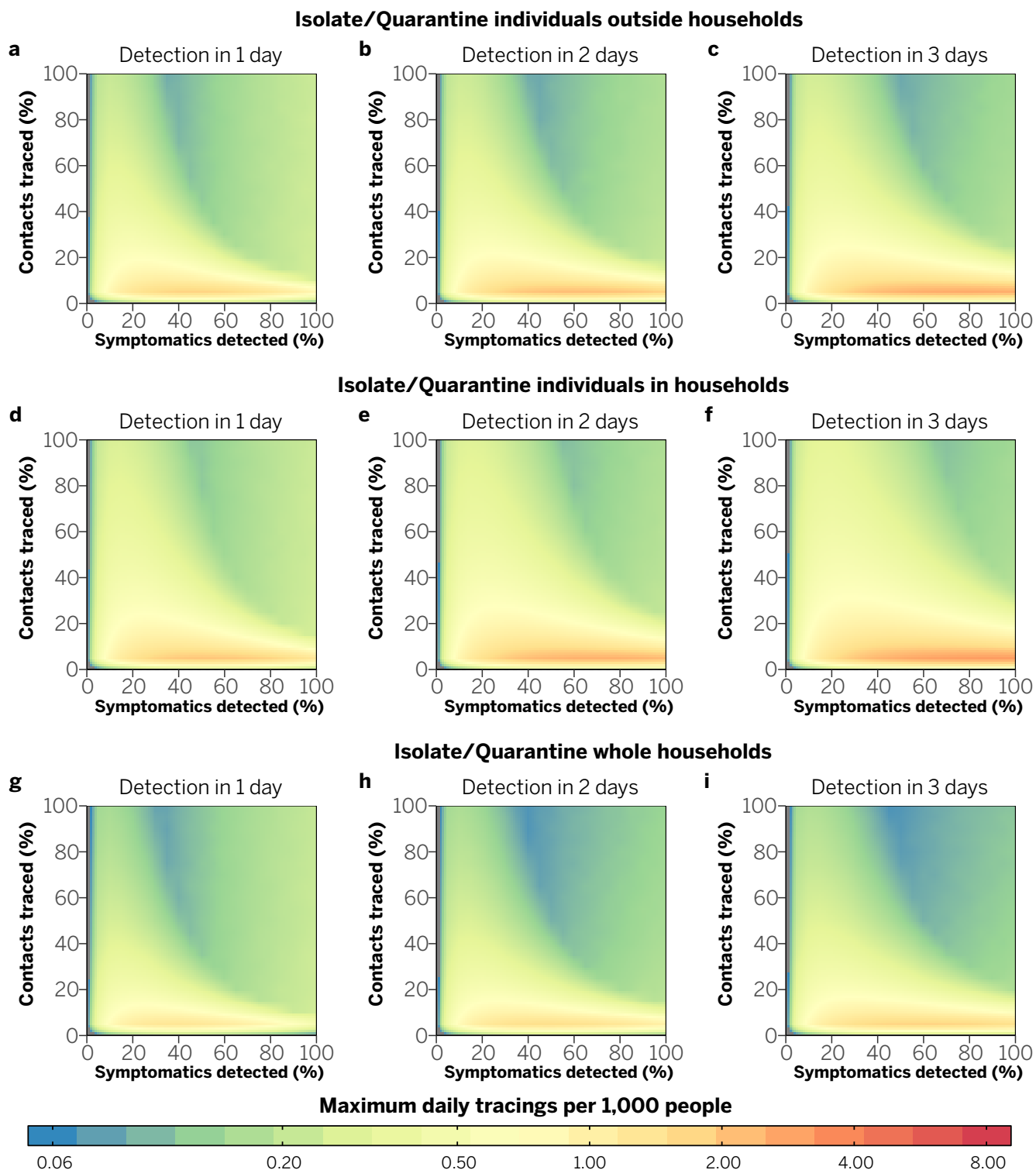
- [1] U.S. Census Bureau. 2018 American Community Survey 5-Year Data (2019). URL <https://www.census.gov/programs-surveys/acs>.
- [2] Foursquare venue categories. <https://developer.foursquare.com/docs/build-with-foursquare/categories/>. Accessed: 2020-04-25.
- [3] Mistry, D. *et al.* Inferring high-resolution human mixing patterns for disease modeling. Preprint at arXiv: <https://arxiv.org/abs/2003.01214> (2020).
- [4] Mossong, J. *et al.* Social contacts and mixing patterns relevant to the spread of infectious diseases. *PLoS medicine* **5** (2008).
- [5] Béraud, G. *et al.* The French connection: the first large population-based contact survey in France relevant for the spread of infectious diseases. *PloS one* **10** (2015).
- [6] Ajelli, M. & Litvinova, M. Estimating contact patterns relevant to the spread of infectious diseases in Russia. *Journal of Theoretical Biology* **419**, 1–7 (2017).
- [7] Zhang, J. *et al.* Patterns of human social contact and contact with animals in Shanghai, China. *Scientific reports* **9**, 1–11 (2019).
- [8] Backer, J. A., Klinkenberg, D. & Wallinga, J. Incubation period of 2019 novel coronavirus (2019-nCoV) infections among travellers from Wuhan, China, 20–28 January 2020. *Eurosurveillance* **25**, 2000062 (2020).
- [9] Nishiura, H. *et al.* Estimation of the asymptomatic ratio of novel coronavirus infections (COVID-19). *International Journal of Infectious Diseases* **94**, 154–155 (2020).
- [10] Verity, R. *et al.* Estimates of the severity of coronavirus disease 2019: a model-based analysis. *The Lancet Infectious Diseases* **20**, 669–677 (2020).
- [11] Ferguson, N. *et al.* Report 9: Impact of non-pharmaceutical interventions (NPIs) to reduce COVID19 mortality and healthcare demand (2020). URL <https://doi.org/10.25561/77482>.
- [12] Kissler, S. M., Tedijanto, C., Goldstein, E., Grad, Y. H. & Lipsitch, M. Projecting the transmission dynamics of SARS-CoV-2 through the postpandemic period. *Science* **368**, 860–868 (2020).
- [13] Du, Z. *et al.* Serial Interval of COVID-19 among Publicly Reported Confirmed Cases. *Emerging Infectious Diseases journal* **26** (2020).
- [14] Ajelli, M. *et al.* Spatiotemporal dynamics of the Ebola epidemic in Guinea and implications for vaccination and disease elimination: a computational modeling analysis. *BMC Medicine* **14**, 1–10 (2016).
- [15] Liu, Q.-H. *et al.* Measurability of the epidemic reproduction number in data-driven contact networks. *Proceedings of the National Academy of Sciences* **115**, 12680–12685 (2018).
- [16] Casey, M. *et al.* Pre-symptomatic transmission of sars-cov-2 infection: a secondary analysis using published data. Preprint at medRxiv: <https://www.medrxiv.org/content/10.1101/2020.05.08.20094870v2> (2020).



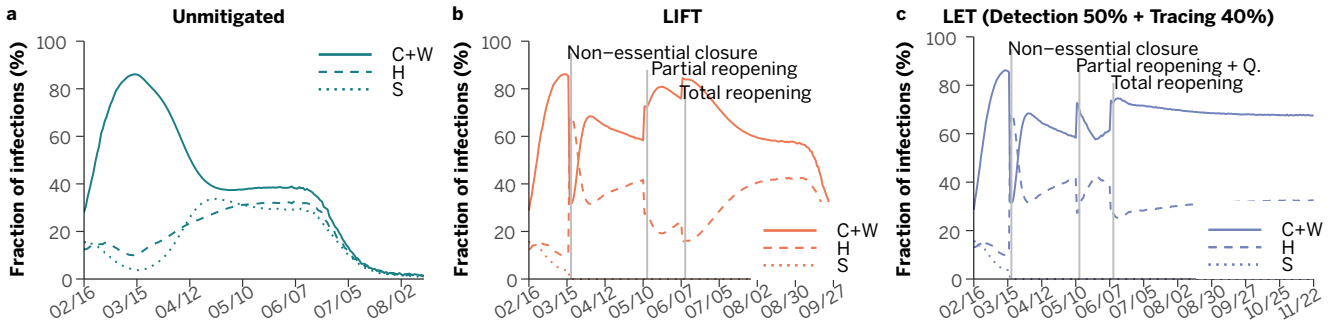
Supplementary Figure 6: Maximum ICU occupation with different isolation/quarantine strategies. From left to right, each column shows the results when the symptomatic individuals are detected and isolated after 1, 2 or 3 days. From top to bottom, each row shows the results for strategies i), ii) and iii). The dashed line indicates when the ICU occupation excess the current availability.



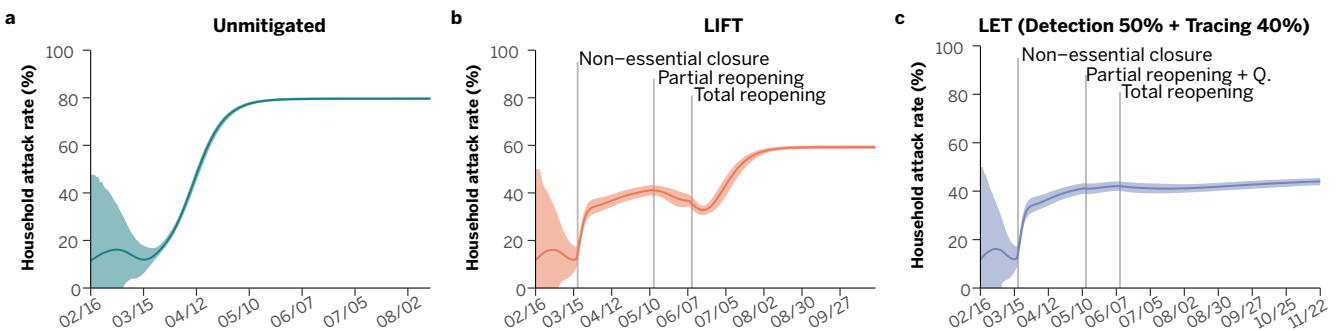
Supplementary Figure 7: Threshold for ICU saturation - with the current estimated ICU availability - as a function of the fraction of symptomatic individuals detected and the fraction of contacts traced. From left to right, we show the results when the symptomatic individuals are detected and isolated after 1, 2 or 3 days.



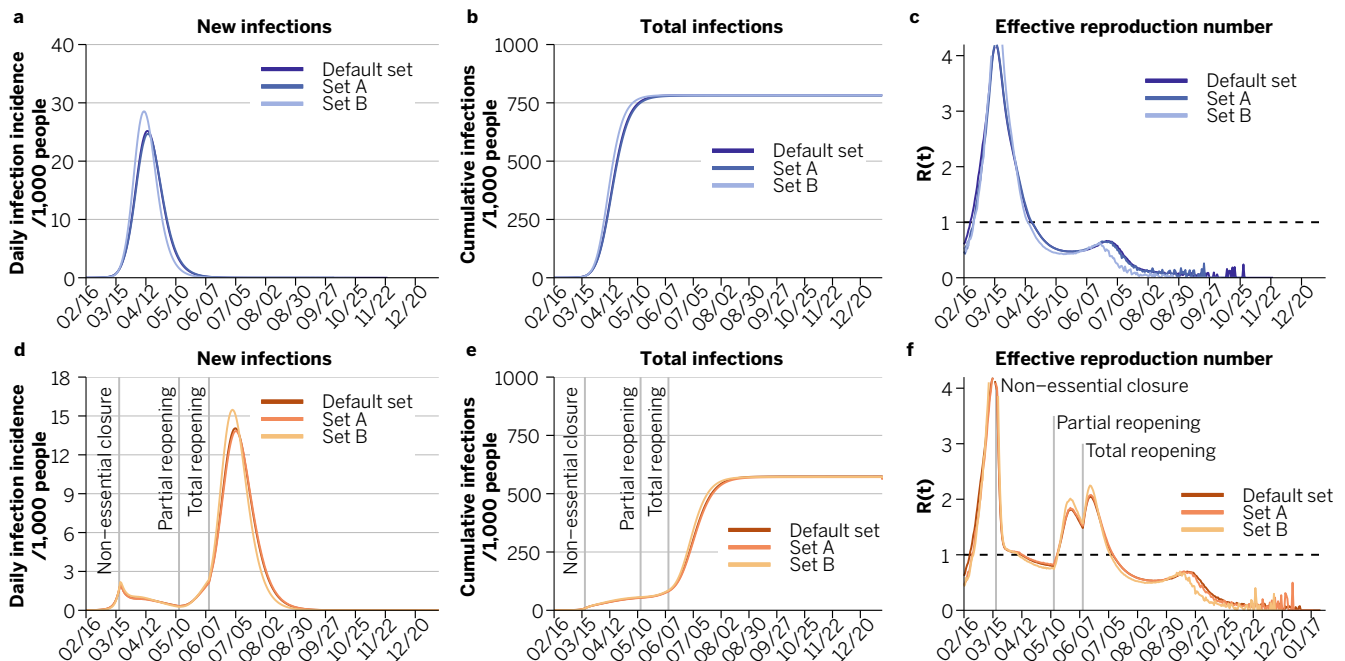
Supplementary Figure 8: Maximum number of individuals whose contacts are traced in a single day per 1,000 people. From left to right, each column shows the results when the symptomatic individuals are detected and isolated after 1, 2 or 3 days. From top to bottom, each row shows the results for strategies i), ii) and iii).



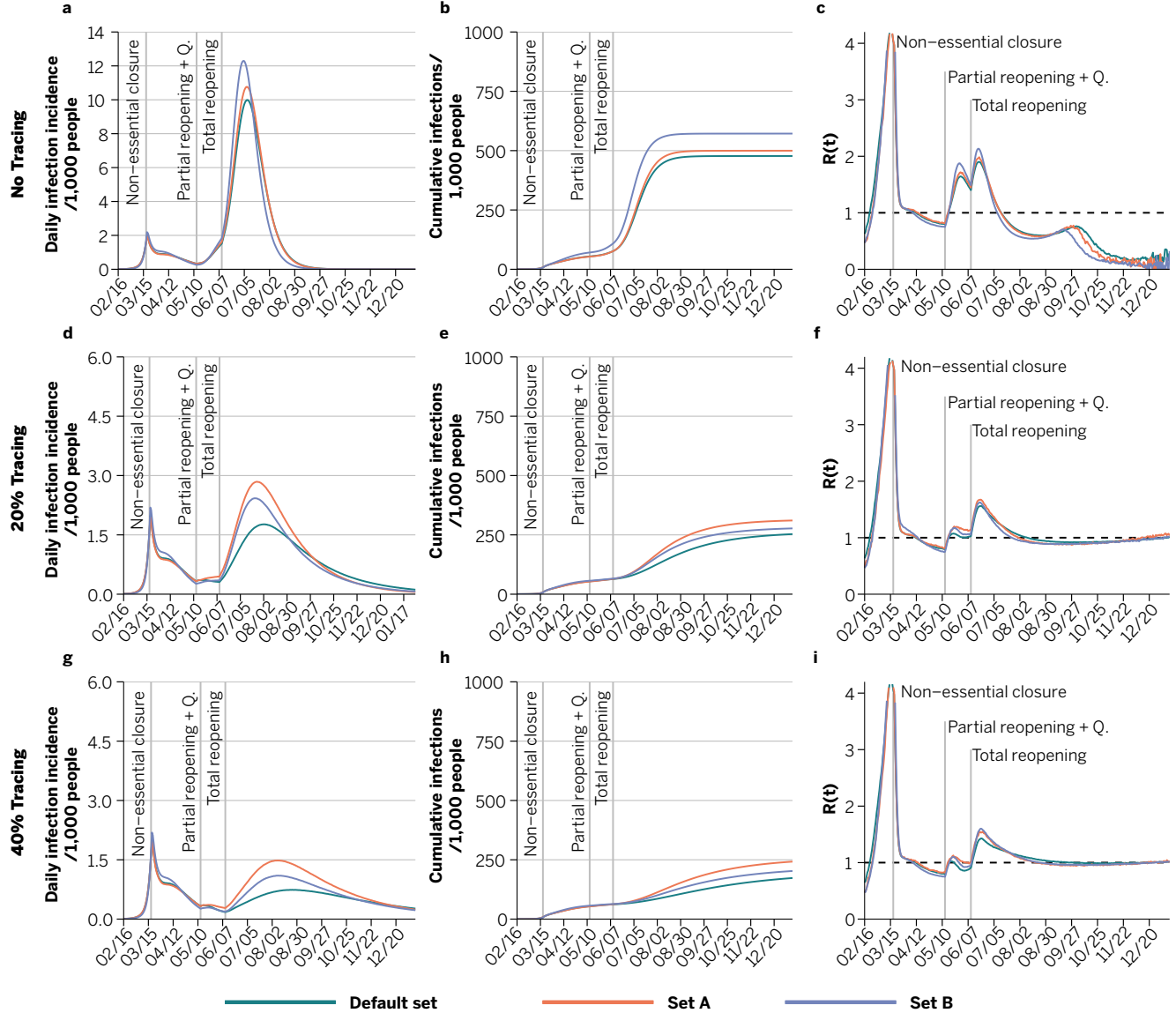
Supplementary Figure 9: Distribution of infections across layers in the unmitigated, LIFT and LET (with 50% detection of symptomatic individuals and 40% tracing) scenarios. Lines represent the average fraction of infections that take place in each layer out of all the infections that have been produced each day.



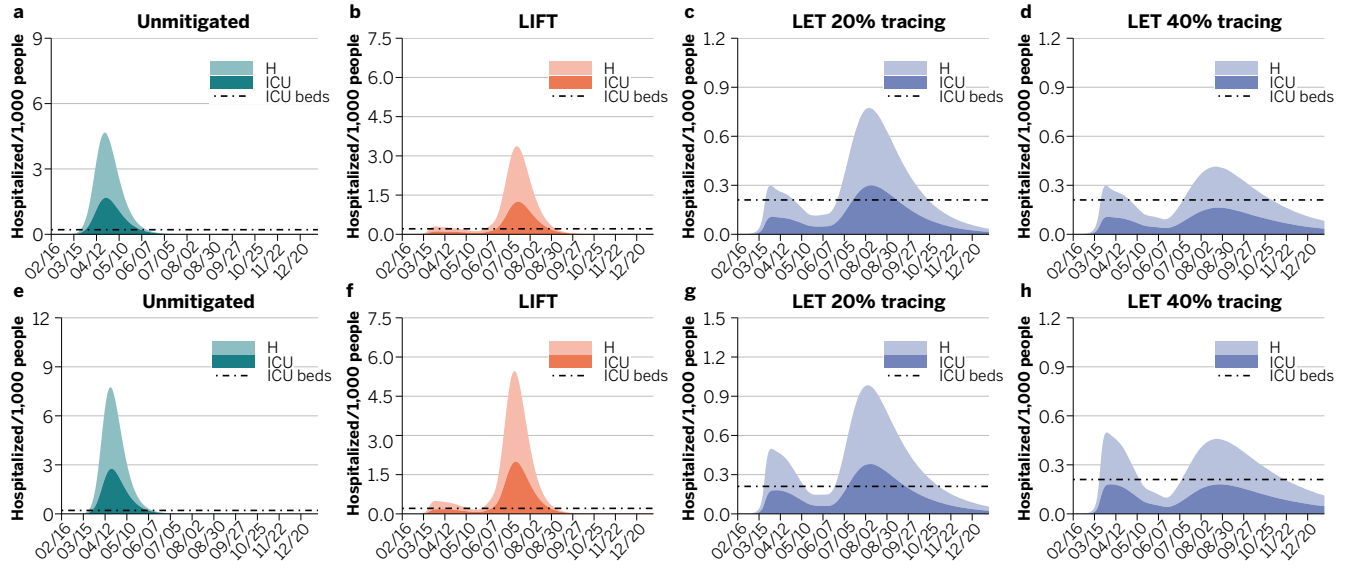
Supplementary Figure 10: Household attack rate as a function of time in the unmitigated scenario, a, LIFT strategy, b, and LET strategy with 50% detection of symptomatic individuals and 40% tracing, c. Solid lines represent the average value while the shaded region shows the 95% C.I.



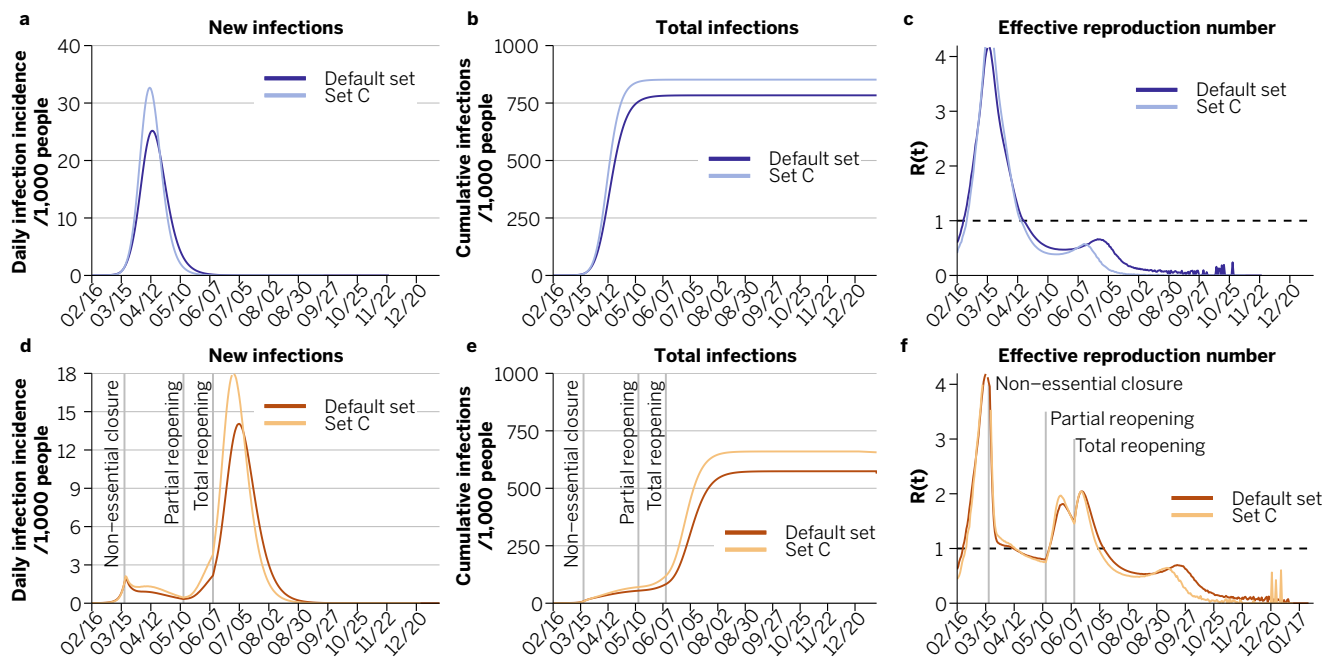
Supplementary Figure 11: Evolution with larger fraction of asymptomatic individuals (set A) and larger pre-symptomatic transmission (set B) for the unmitigated scenario and LIFT strategy.



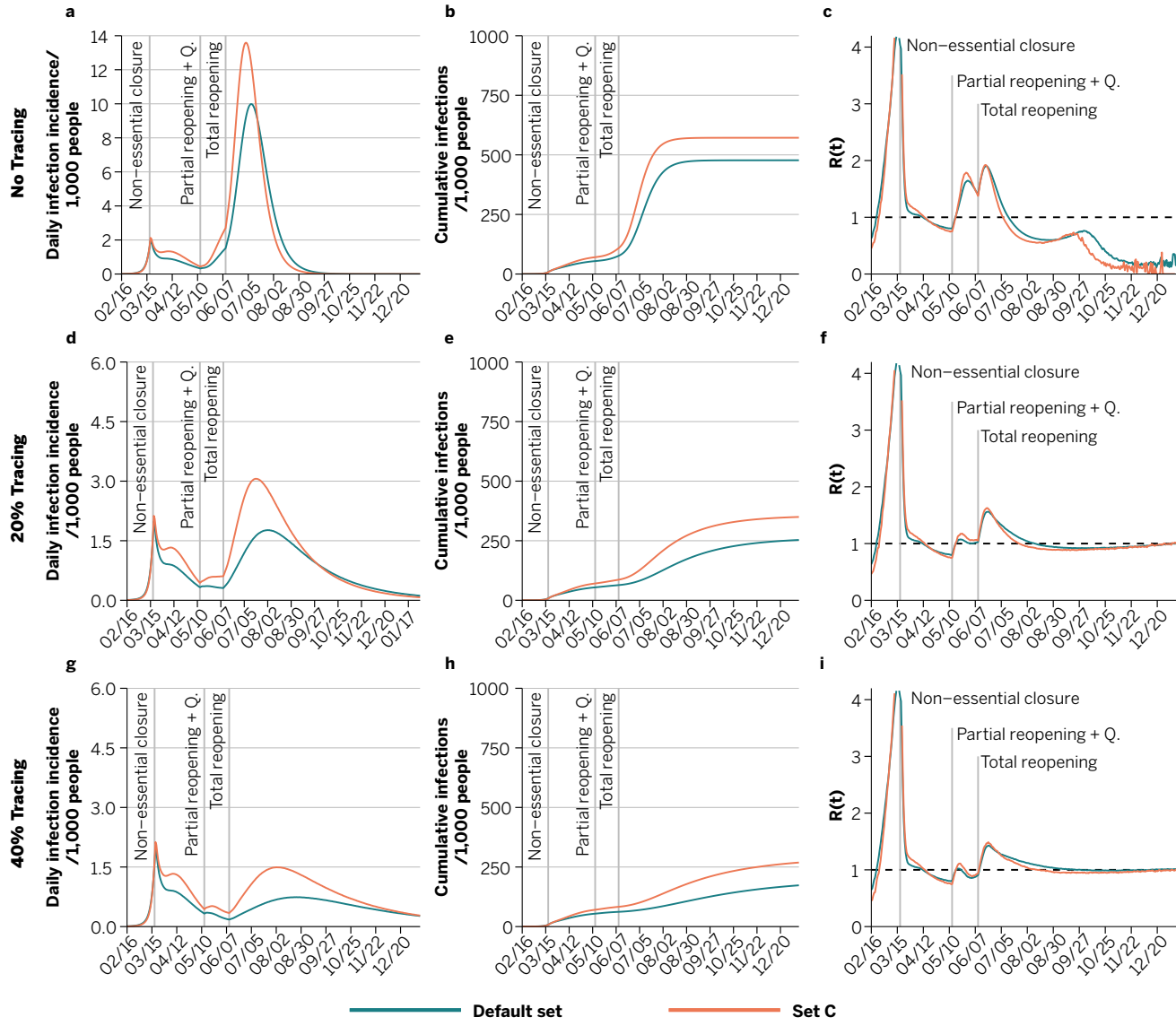
Supplementary Figure 12: Evolution with larger fraction of asymptomatic individuals (set A) and larger pre-symptomatic transmission (set B) for the LET scenario with 50% of symptomatic detection. The top, mid and bottom rows show the results with 0%, 20% and 40% of tracing, respectively.



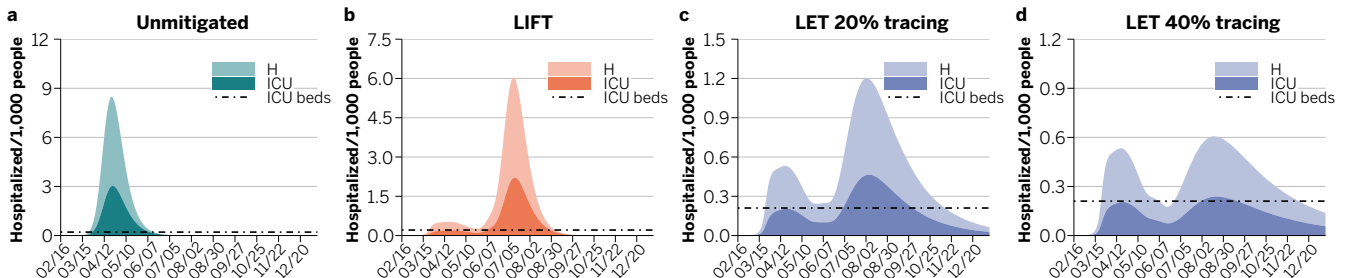
Supplementary Figure 13: Evolution of the hospitalizations. Top row: set of parameters A (50% of asymptomatic individuals). Bottom row: set of parameters B (fraction of pre-symptomatic transmission  $k = 0.50$ ).



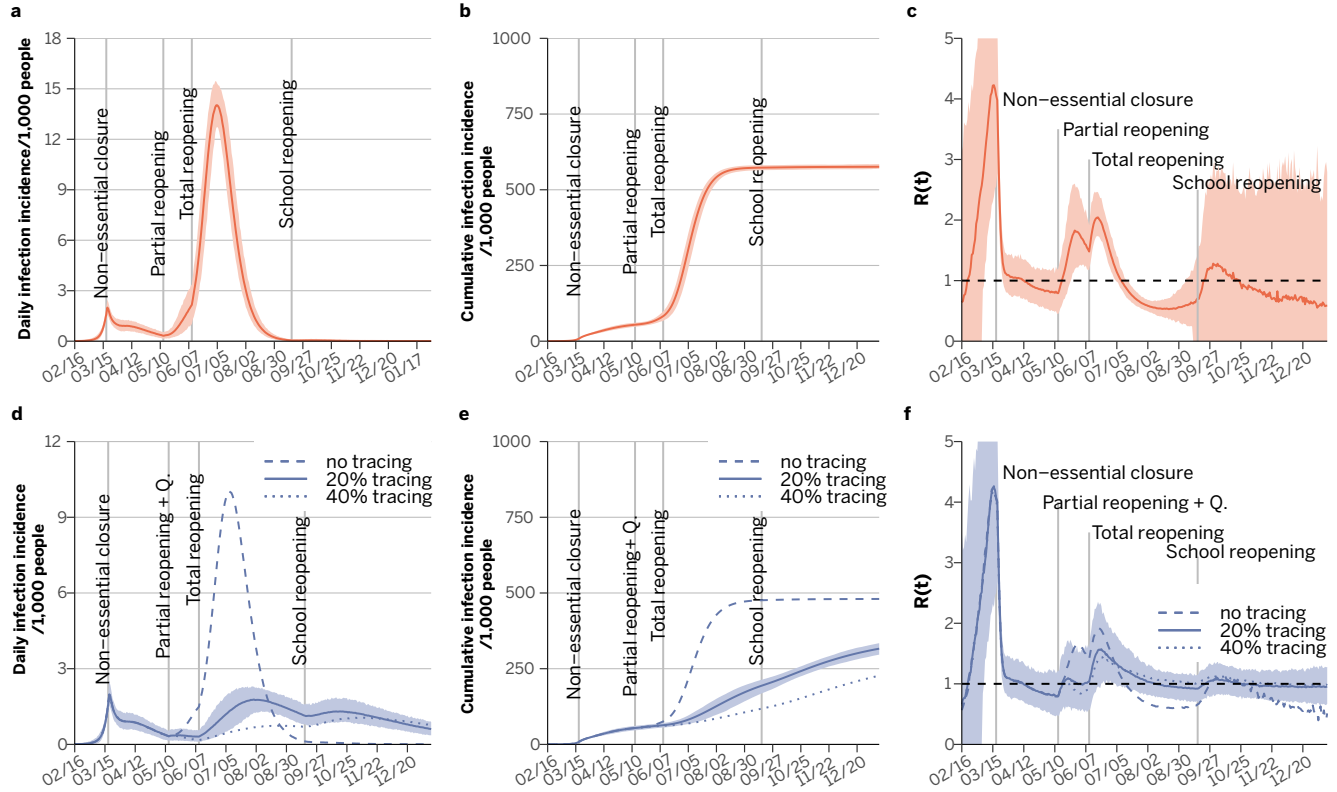
Supplementary Figure 14: Evolution with larger  $R_0$  (set C) for the unmitigated scenario and LIFT strategy.



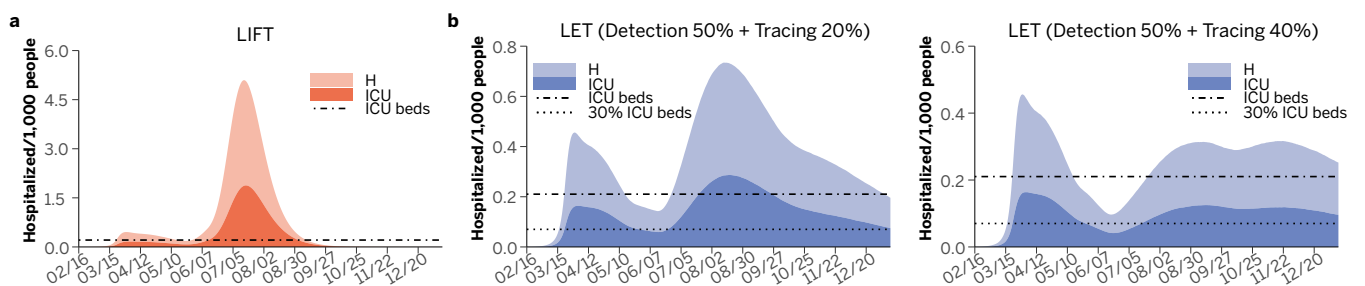
Supplementary Figure 15: Evolution with larger  $R_0$  (set C) for the LET scenario with 50% of symptomatic detection. The top, mid and bottom rows show the results with 0%, 20% and 40% of tracing, respectively.



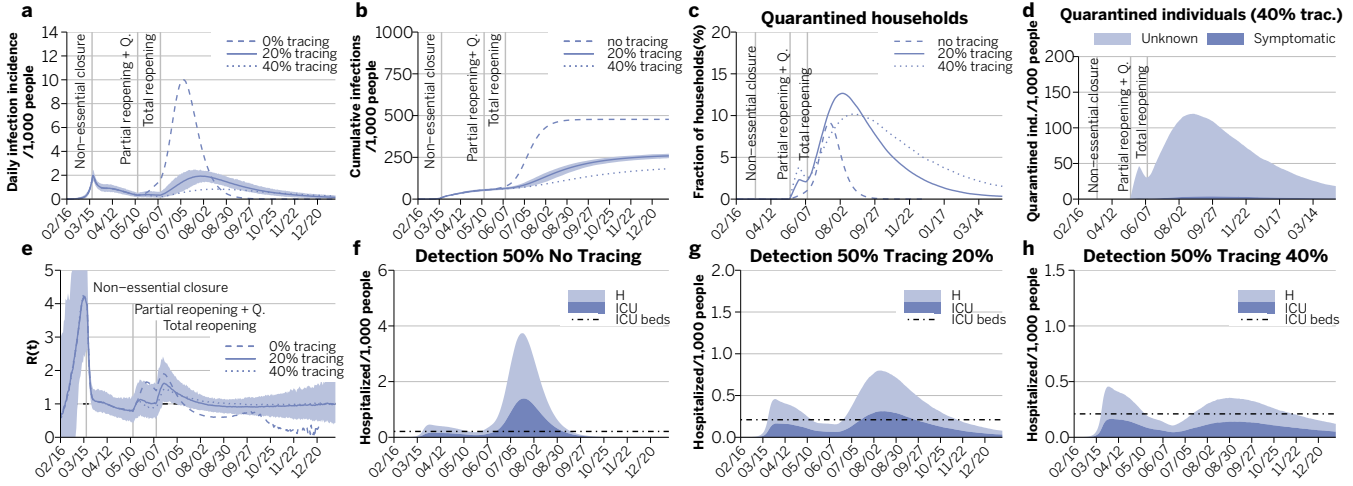
Supplementary Figure 16: Evolution of the hospitalizations with larger  $R_0$  (set C).



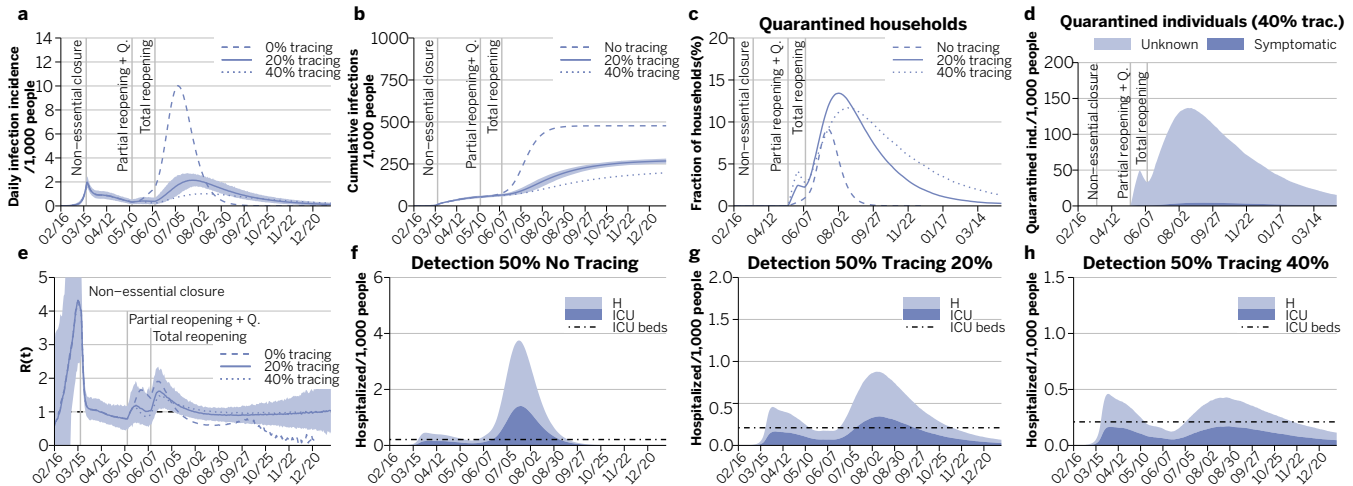
Supplementary Figure 17: Evolution of the system when 30% of the symptomatic individuals are isolated at their homes and their contacts traced and quarantined in their households, default set of parameters.



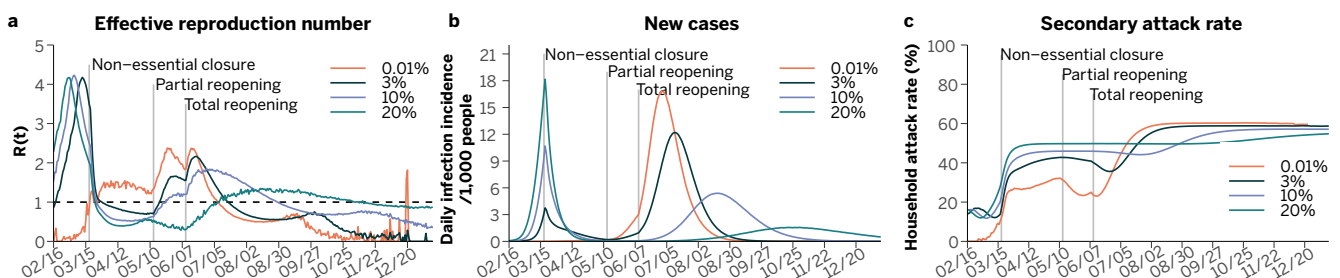
Supplementary Figure 18: Evolution of the system when 70% of the symptomatic individuals are isolated at their homes and their contacts traced and quarantined in their households, default set of parameters.



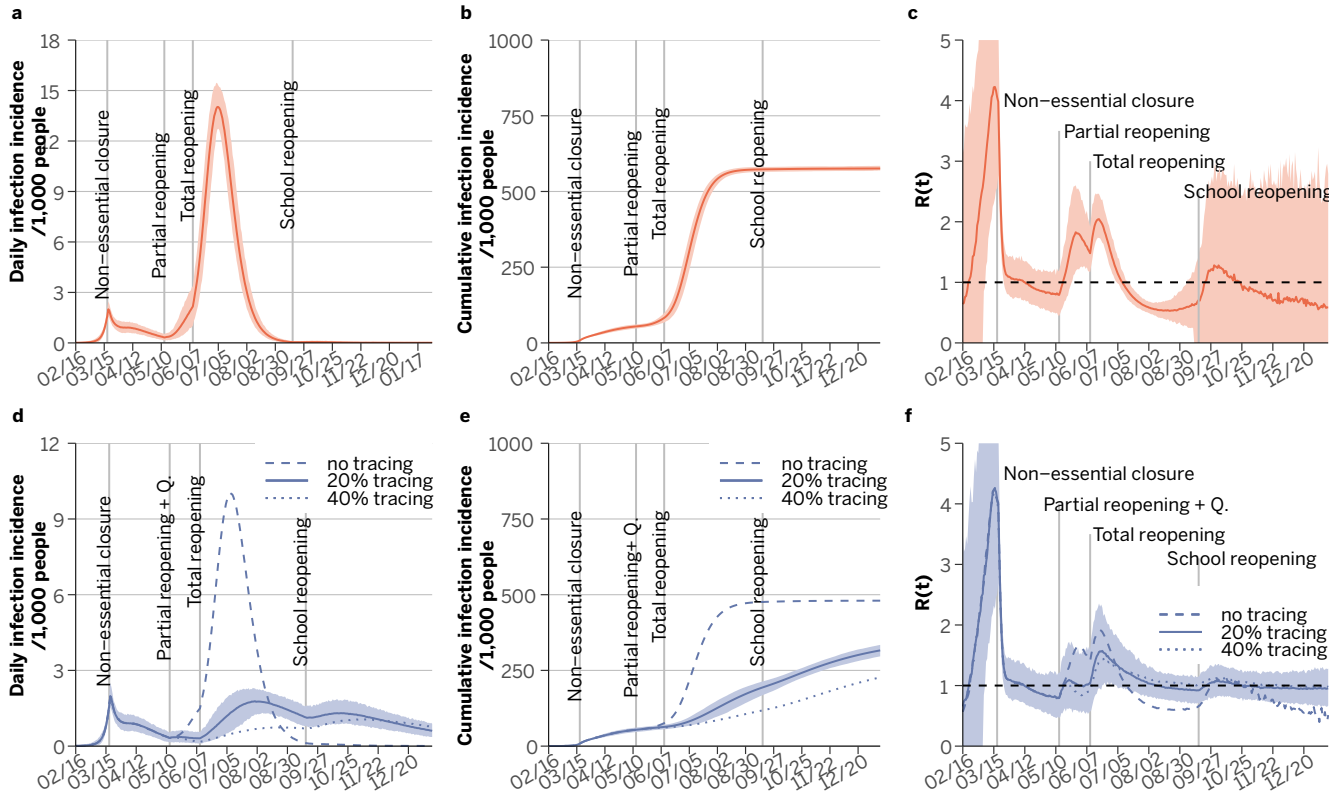
Supplementary Figure 19: Evolution of the system when there is a 1 day delay between the isolation of a symptomatic individuals and the tracing and isolation of its contacts.



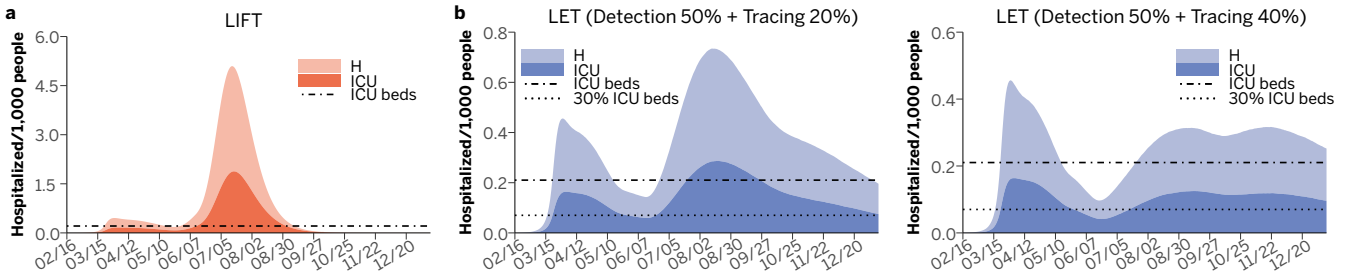
Supplementary Figure 20: Evolution of the system when there is a 2 days delay between the isolation of a symptomatic individuals and the tracing and isolation of its contacts.



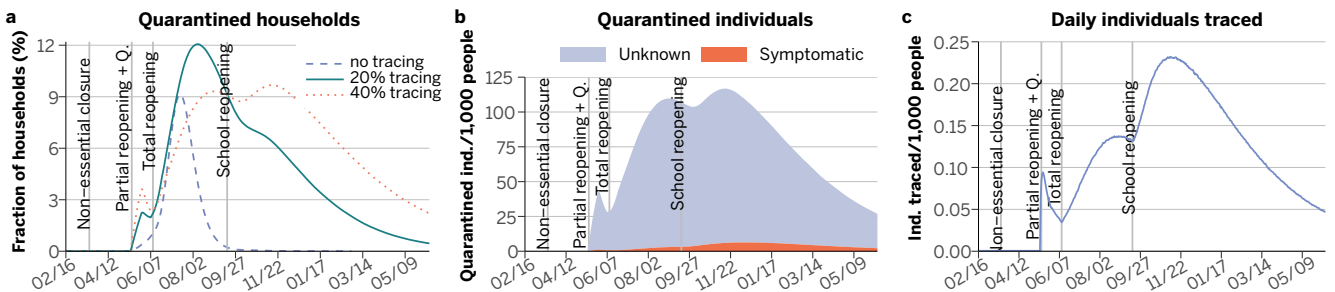
Supplementary Figure 21: Effective reproduction number, daily incidence and household attack rate for different initial attack rates. The sooner the intervention, the larger the second wave can be.



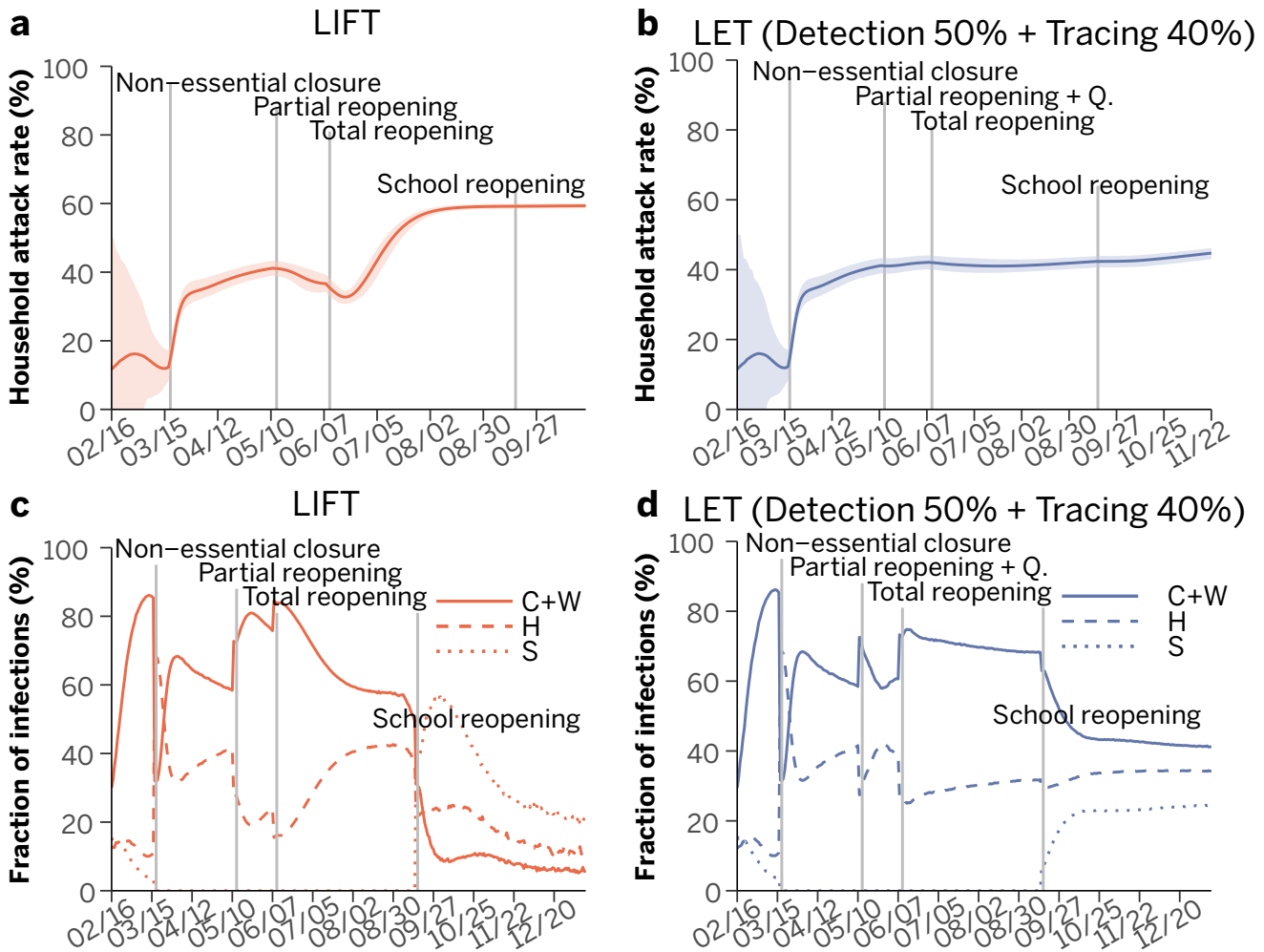
Supplementary Figure 22: Evolution of the LIFT and LET scenarios when schools are reopened on the 15th of September.



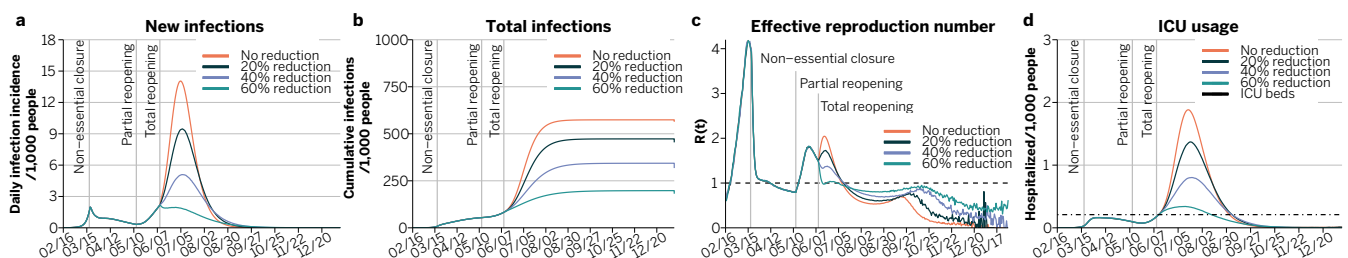
Supplementary Figure 23: Evolution of hospitalizations in the LIFT and LET scenarios when schools are reopened on the 15th of September.



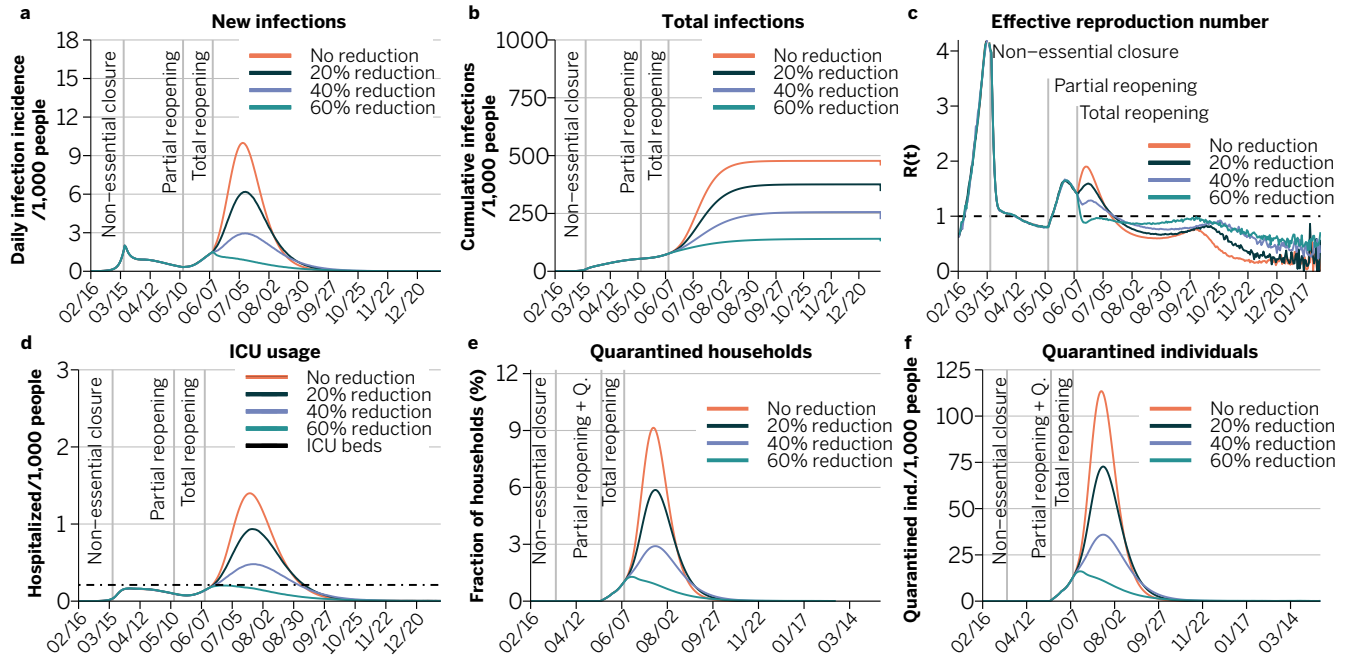
Supplementary Figure 24: Affordability of the quarantine strategy when schools are reopened on the 15th of September.



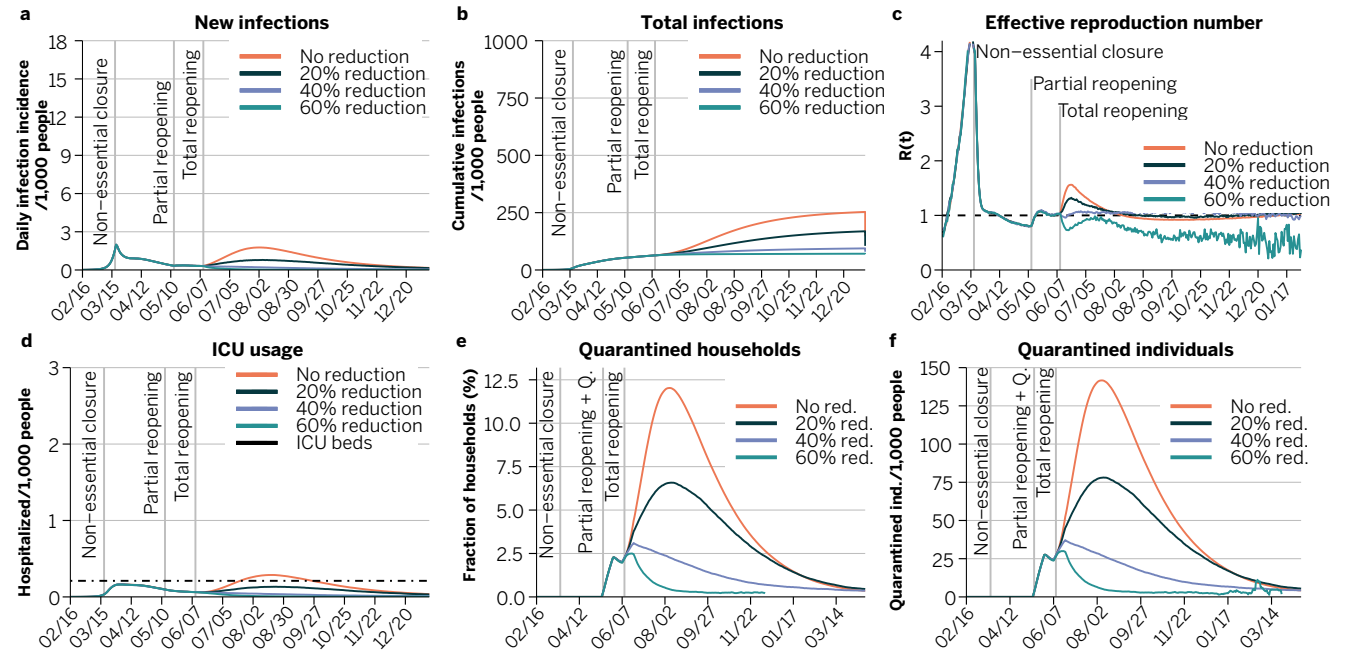
Supplementary Figure 25: Household attack rate (**a, b**) and fraction of infections that take place in each setting (**c, d**) when schools are reopened on the 15th of September.



Supplementary Figure 26: Evolution of the system under the LIFT scenario when the transmissibility is reduced by 20, 40 or 60%.



Supplementary Figure 27: Evolution of the system under the LET scenario when the transmissibility is reduced by 20, 40 or 60%, with 50% symptomatic detection and isolation but without tracing.



Supplementary Figure 28: Evolution of the system under the LET scenario when the transmissibility is reduced by 20, 40 or 60%, with 50% symptomatic detection and isolation and tracing of 20% of the contacts.